

Geological Society, London, Special Publications

## **LiDAR basics for natural resource mapping applications**

James D. Giglierano

*Geological Society, London, Special Publications* 2010; v. 345; p. 103-115  
doi: 10.1144/SP345.11

---

### **Email alerting service**

click [here](#) to receive free e-mail alerts when new articles cite this article

### **Permission request**

click [here](#) to seek permission to re-use all or part of this article

### **Subscribe**

click [here](#) to subscribe to Geological Society, London, Special Publications or the Lyell Collection

---

### **Notes**

**Downloaded by** on October 12, 2011

---

# LiDAR basics for natural resource mapping applications

JAMES D. GIGLIERANO

*Iowa Geological Survey, Iowa Department of Natural Resources, 109 Trowbridge Hall,  
Iowa City, IA 52242-1319, USA (e-mail: james.gigliero@dnr.iowa.gov)*

**Abstract:** LiDAR elevation data is becoming widely available for use by many non-engineering mapping specialists such as geologists, soil scientists and planners. Understanding the basics of LiDAR data acquisition is essential to using the data effectively in mapping applications, including how vegetation affects the vertical accuracy of LiDAR. Tools are available for mapping specialists to process raw LiDAR data into useful GIS products so they do not have to rely on vendor supplied products.

The purpose of this paper is to help newcomers understand the basics of Light Detection And Ranging (LiDAR) data collection and processing, especially non-engineering, mapping specialists such as geologists, soil scientists and those interested in land cover characterization. LiDAR is being increasingly used worldwide for the collection of detailed elevation data. In the USA many states are embarking on large-scale LiDAR acquisitions, and inevitably LiDAR elevation and other derived products will become widely available to many different audiences. To make full use of this new source of information a knowledge of LiDAR data collection and handling procedures will be required, as well as guidance for the conversion and utilization of vendor-supplied files. In some cases mappers may have to perform the processing themselves, or may ask for this to be done by vendors or third parties. In other cases, LiDAR-derived topographical data may be supplied by a local government entity that has no metadata, and in these instances the user will have to make some assumptions about the type of processing that may have been performed.

## How LiDAR data is collected and represented

The LiDAR equipment basically consists of a laser rangefinder operating from some form of airborne platform (helicopter, plane or satellite) that makes repeated measurements of the distance from the platform to the ground. The position and elevation of the platform is precisely known, using airborne GPS along with ground control, so that the elevation of the ground surface can be calculated by subtracting the laser rangefinder distance from the height of the platform. Compensation must be made for the tilt and pitch of the airborne platform using

gyroscopes and accelerometers in the aircraft's inertial measurement unit. A good technical overview of LiDAR scanning technology is provided by Wehr & Lohr (1999).

LiDAR systems record thousands of highly accurate distance measurements every second (newer systems up to 150 kHz; older systems 30–80 kHz) and create a very dense coverage of elevations over a wide area in a short amount of time. Because LiDAR is an active sensor that supplies its own light source, it can be used at night thus avoiding routine air traffic. It can also be flown under some types of high cloud conditions. Most LiDAR systems record multiple surface reflections, or 'returns', from a single laser pulse. When a laser pulse encounters vegetation, power lines or buildings, multiple returns can be recorded. The first return will represent the elevation near the top of the object. Second and third returns may represent trunks and branches within a tree, or understorey vegetation. Hopefully, the last return recorded by the sensor will be the remaining laser energy reflecting off the ground surface, but sometimes the tree blocks all the energy from reaching the ground. These multiple returns can be used to determine the height of trees or power lines, or give indications of forest structure (crown height, understorey density, etc.). Figure 1 shows a single 2 × 2 km tile consisting of 3.3 million first return LiDAR points.

Another feature of an airborne LiDAR system is the use of mirrors or other technology to point the laser beam to either side of the aircraft as it moves along its flight path. Depending on the scanning mechanism, the LiDAR scans can have a side-to-side, zig-zag, sinusoidal or wavy pattern. While the laser itself pulses many thousands of times per second, the scanning mechanism usually moves from side to side at around 20–40 cycles s<sup>-1</sup>. This scanning, combined with the

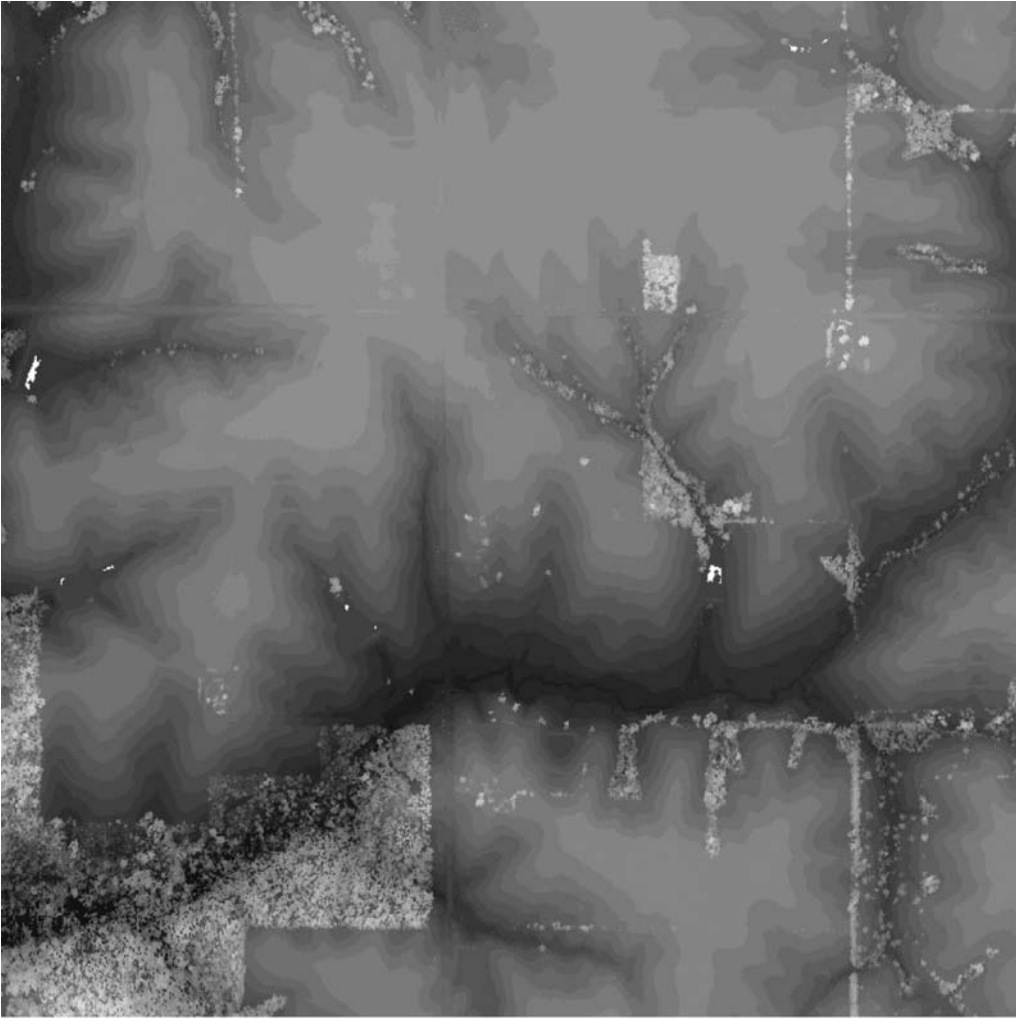


**Fig. 1.** Grey scale image consisting of 3.3 million LiDAR first return LiDAR points. First returns indicate the tops of trees and buildings, as well as bare ground in open areas. White areas are data voids where no returns were recorded, usually from non-reflecting water surfaces.

forward motion of the aircraft, produces millions of elevations in a short distance and time. The field of view or angle the scan makes from side to side can be adjusted by the operator, but usually is  $30^{\circ}$ – $40^{\circ}$ . This creates a swathe of around 1 km in width or less. Adjacent swathes overlap by 15–30% so that no data gaps are left between flight lines.

The spacing of LiDAR points on the ground is a function of the laser pulse frequency, scan frequency and flight height (Baltsavias 1999). While there is usually a nominal or average point spacing specified in a LiDAR project, actual data points have variable spacings that are smaller and larger

than the specified spacing. Mappers need to be aware of these effects when viewing final products that were derived from the raw data. The second aspect is that because the laser scans from side to side, it interacts with the ground in different ways depending on the angle of incidence. LiDAR pulses at the edge of a scan will strike the sides of buildings, whereas pulses at the centre of a scan will only strike the tops of roofs. Likewise, pulses at the edges of scans will pass through trees at an angle. Sometimes this will create ‘shadows’ on the other side where no LiDAR passes through. In addition, less energy will return to the LiDAR

receiver as it reflects away from the aircraft. This is evident in the images created from the intensity values for each return: one can see overall darkening of the intensity at the edges of swathes. The latter appear darker than the returns at the centre of swathes.

### How LiDAR points are processed into TINs and DEMs

In the spring of 2005 the Iowa Department of Natural Resources (DNR) and others acquired LiDAR coverage with a nominal resolution of 1 m over the Lake Darling watershed from a commercial vendor. The vendor's LiDAR system collected a first and last return from each LiDAR pulse. From the first and last returns a so-called 'bare earth' return was created using a proprietary classification algorithm developed by the vendor. Such classification systems try to sort out non-bare earth returns (tree tops, buildings, power lines, vehicles) from bare earth (ground surface) returns. They use differences in elevation between the first and last returns, relative changes in elevation and slope to distinguish bare earth in forested areas. Intensity data are used to identify vegetation and man-made materials. The LiDAR data for the Lake Darling watershed was collected in April, before most trees and bushes had leaves. There are some data voids in forested areas owing to non-penetration of the laser through the tree canopy, but these areas are generally less than 10 m across and are easily filled in by interpolation. Leaf-on conditions and tall crops, such as corn, do not allow easy penetration of the laser beam to the ground and should be avoided.

LiDAR data for the Lake Darling area came from the vendor in the form of  $2 \times 2$  km tiles with  $x$  and  $y$  co-ordinates,  $z$  elevations and intensity values in ASCII text format. With a nominal 1 m posting spacing, some tiles had up to 3.3 million points. Points near the centre of the flight lines were close to the nominal 1 m spacing (Fig. 2), while towards the ends of scans the points converge with the start of the next scan (Fig. 3). In this dataset the scanning pattern was a zig-zag, which made some points converge while others diverged. The points can be less than half of the nominal spacing and, likewise, where they diverge they can be twice the nominal spacing. Because some points can be as close as 0.5 m, the tiles were initially interpolated to create grids with 0.5 m resolution, the idea being that no data points should be merged or averaged with any other points. There is a tendency among some users to create grids with resolutions of 3, 5 and even 10 m in order to save storage space, or as a way to reduce the volume of data to process. We

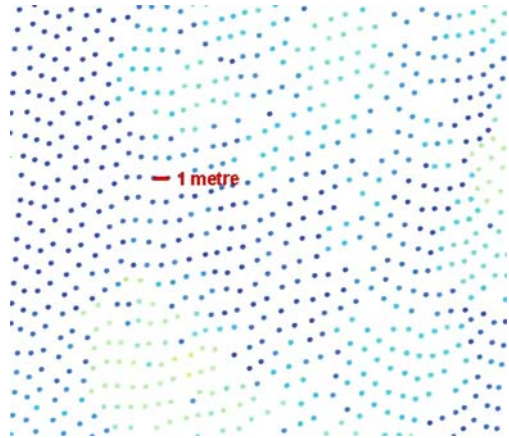


**Fig. 2.** An area in the middle of a LiDAR flight line. LiDAR point spacing is around 1 m at the centre of back-and-forth scans.

desired to create the grids as close as possible to the native resolution of the LiDAR data in order to fully evaluate its potential to represent the smallest surface features.

To make digital elevation models (DEM) from the tiles, the Surfer 8 software (<http://www.goldensoftware.com/products/surfer/surfer.shtml>) was used. This software first creates a TIN (triangulated irregular network) before it interpolates the points into a raster DEM. However, once the DEM tiles were initially put together into mosaics, it

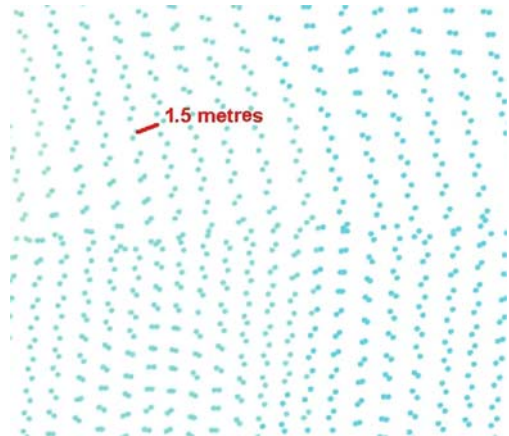


**Fig. 3.** An area of two adjacent LiDAR flight lines. The point spacing is highly variable at the edges of flight lines. Some points are less than 1 m apart at the end of one and beginning of the next scan, while the distance between points in different sets of scans can be as much as 1.5 m apart.

became obvious that there were noticeable gaps between each tile. To remedy this problem a short C program was created to sort through the ASCII text files of the adjacent tiles and find points within a 3 m buffer of the edge of the tile to be processed. The tiles were then reprocessed, adding the 3 m buffers, and when these raster tiles were merged together into a mosaic the gaps were almost completely eliminated. Leica Imagine (<http://gi.leica-geosystems.com/>) software was used to mosaic all the tiles into one large raster DEM file. From the DEM, shaded relief images were created and compressed. Digital elevation models and shaded relief images were then easily imported into ArcGIS software (<http://www.esri.com/>) for display and further analysis.

Field examination of the LiDAR bare earth shaded relief images was conducted in January 2006. It was surprising how well the LiDAR shaded relief images represented the smallest topographical features, including small slope changes of less than 0.5 m, even in forested areas. There were some data voids, owing to the lack of penetration through the dense tree canopy, but there were

enough data points to show good definition of incised stream channels, meander scars and gullies (Fig. 4). Man-made features such as road ditches and embankments, terraces and dams were also well defined. Tillage patterns are evident as regular lineated textures on crop fields.

Because the bare earth processing does not remove 100% of the forest artefacts, a distinctive bumpy pattern remains in the bare model that indicates the presence of forest cover (Fig. 5). During field examination it was noticed that different canopy structures were represented by different patterns in the artefacts. In the tall-canopy floodplain forest most of the bumps were removed leaving a predominantly smooth surface, whereas on side slopes with a thick understorey or brush cover the texture on the shaded relief image is rougher in appearance. Interestingly, the bare earth processing removed nearly all of the numerous tree falls in the stream channels, which allows drainage tracing programs to work well when following flow paths downstream. Also, areas with pine trees were very smooth, indicating nearly complete penetration of the laser beam.

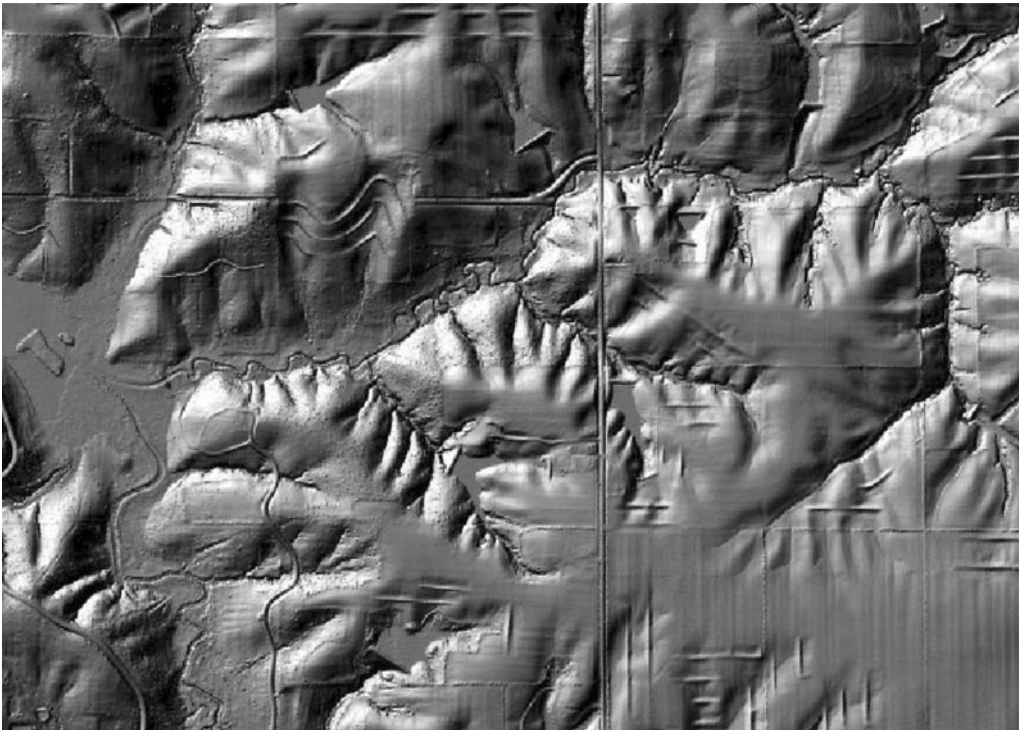


**Fig. 4.** Portion of the bare earth shaded relief image of the Lake Darling watershed showing natural and man-made features readily apparent in the LiDAR data. Natural and man-made drainage features, roadbeds, fence lines and tillage patterns are readily visible.

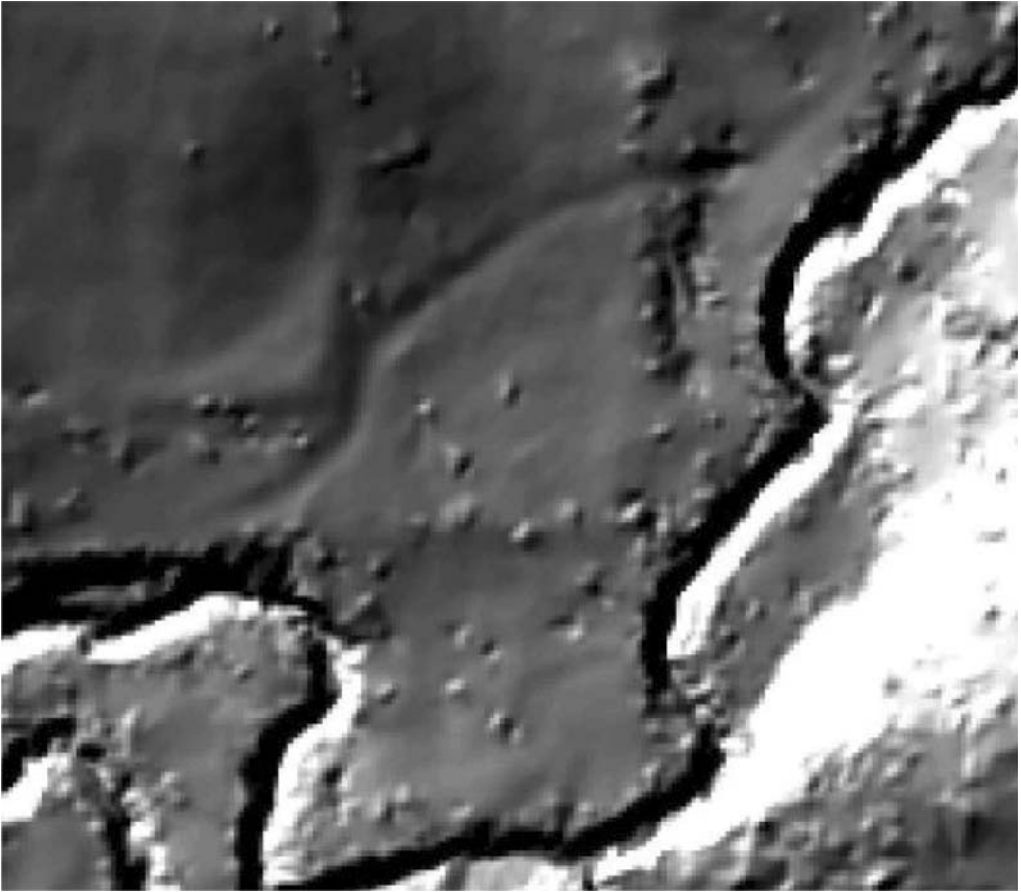


**Fig. 5.** Portion of a bare earth shaded relief image showing artefacts (bumpy texture) in deciduous forest areas. These artefacts are LiDAR elevations classified as bare earth, but probably are from tree trunks, branches or understorey close to the ground and classified as bare earth by the vendor's algorithm.

### How to use LiDAR products for mapping applications

Once the raw LiDAR point tiles are processed into high-resolution DEMs, other useful mapping products can be derived. The derived shaded relief image previously mentioned (Fig. 4) is very useful for visual display and interpretation, and can be combined with colourized elevation images for extra information content. Another useful display product is the slope map, which can be derived from the DEM using the grid processing tools found in almost every GIS package. Usually a choice can be made as to whether the slope rate is calculated in degrees or as percentages ( $45^\circ$  slope = 100%). A slope map based on percentage can be grouped into the slope classes typically used by soil survey mappers (A slope class = 0–2%, B = 2–4%, etc.), and can be readily compared

to soil polygons displayed by slope class (Fig. 6). Figure 7 shows the new level of detail available in slope classes derived from LiDAR data.

Besides the elevation component of the LiDAR return, many systems produce an intensity component that indicates the strength of the LiDAR return. This intensity value is mostly influenced by the reflectance of the material struck by the laser pulse, but is also influenced by the scan angle (laser pulses directed away from the airplane at significant angles do not reflect back as much light energy as a pulse directed straight down from the plane). Because most LiDAR systems use a laser that emits light in the near-infrared portion of the spectrum (LiDAR used for Lake Darling had a wavelength of 1064 nm), the intensity of LiDAR return is directly related to the near-infrared reflectance of the target material. An image constructed from the intensity component of the returns looks

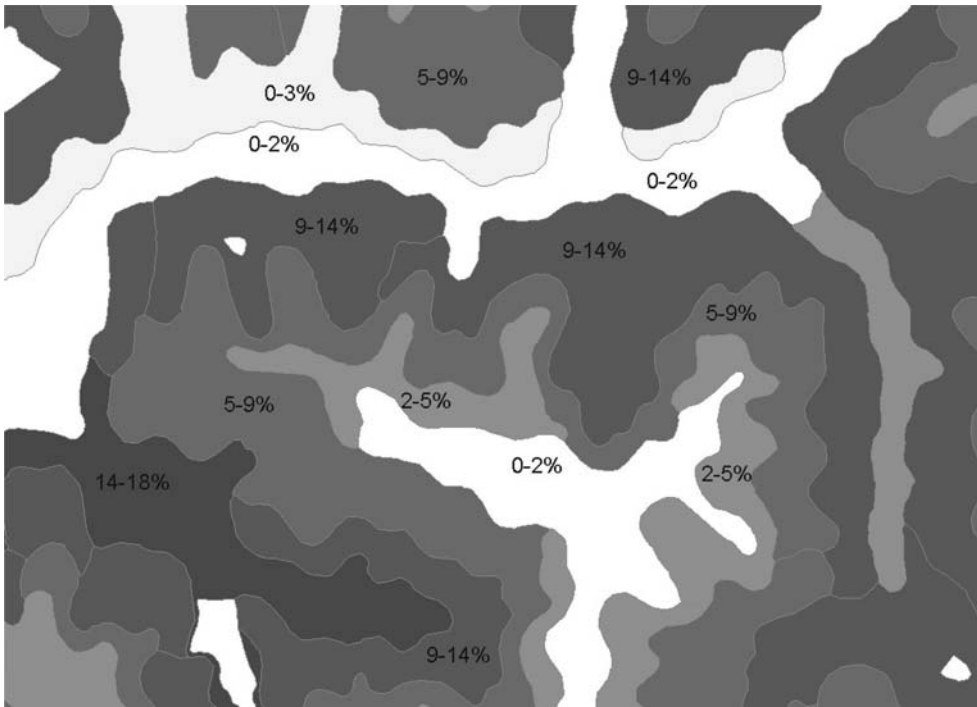


**Fig. 6.** Soil survey soil polygons shaded by slope class range: light shades are lower slopes and darker shades indicate steeper slopes.



**Fig. 7.** Slope class ranges derived from Lake Darling LiDAR data. While low slope areas on LiDAR look similar to the soil polygons, LiDAR more clearly represents steep slopes such as gullies and stream channels.



**Fig. 8.** Portion of a LiDAR intensity image of the Lake Darling watershed, constructed from bare earth return intensity values.

very much like a black and white near-infrared aerial photograph (Fig. 8). An intensity image has one interesting peculiarity, however: tree shadows point away from the flight lines, so one can see shadows pointing in opposite directions close together at the edge of two flight lines. Because intensity is recorded from each LiDAR return, it is possible to construct first return intensity images as well as last return intensity images, and have them look quite different, especially in forested areas where the first return might represent mainly the tree tops but the last return intensity could represent many other features, including the forest floor.

### **Vertical accuracy test and influence of land cover**

Usually one of the first questions asked by new LiDAR users concerns the vertical accuracy of the elevation data. In the Lake Darling project the stated accuracy is 15 cm (0.5 ft) RMSE (root mean square error) in the bare earth areas and 37 cm (1 ft) in vegetated areas. Because there are no high

accuracy geodetic monuments in the watershed, and we did not have access to survey grade GPS equipment, we needed some other way to test the vertical accuracy. Fortunately, a digital terrain model and associated 2 ft contours produced by aerial photography and photogrammetric techniques for a road project was available from the Washington County Engineer's office. The digital terrain model and contours were created by a local aerial photography firm, and had a stated vertical accuracy of 6.1 cm (0.2 ft). The area covered by the model is over 3.2 km (2 miles) long and 0.4 km (0.25 mile) wide. The digital terrain model consisted of elevation points and break lines (Fig. 9) in CAD format. Using the 3D\_ANALYST extension in ArcGIS, the photogrammetrically derived terrain model was converted into a triangulated irregular network or TIN, and interpolated into a 1 m elevation grid. The LiDAR elevation grid was then subtracted from the photogrammetry grid to produce a simple difference grid: the overall average difference between the two grids was only 3.3 cm (0.11 ft). In order to compare the two grids to their stated accuracies, the RMSE had to be calculated. First, the simple difference grid was



**Fig. 9.** A  $0.4 \times 0.6$  km portion of shaded relief of a digital terrain model derived from low-altitude aerial photographs. The black dots are elevation mass points and the black lines are break lines.

multiplied by itself to create the squared difference grid. Using a polygon coverage of land cover from 2005, the mean squared difference was calculated for each land cover class using the zonal statistics command in ArcToolBox. By using the spatial calculator function in the SPATIAL\_ANALYST extension, the square root of the values in the 'mean' field of the table, the RMSE, was found for each land cover class. The zonal statistic tool also computes a 'count' of cells for each class and a 'sum' of the elevations within that class. Calculating

the sum of all the 'count' field values and 'sum' field values for all the classes, and dividing the total sum by the total count found the average squared difference for the entire dataset. By taking the square root of this value, the RMSE was found for the whole area. Initially, RMSE between the LiDAR DEM and the photogrammetry DEM was found to be 0.79 ft or 24.1 cm.

Upon examination of the squared difference image, it was apparent that the terrain in several areas had changed significantly between the time

OID	LAND_USE	ZONE_C	COUNT	AREA	MIN	MAX	RANGE	MEAN	STD	SUM	RMSE_ft	RMSE_CM
0	Residential	1	36665	36665	0.00000	18.04	18.04	0.262028	0.823366	9607.27	0.511887	15.8023
1	Water	2	26069	26069	0.00000	10.053	10.053	0.234739	0.848544	6119.4	0.484499	14.7675
2	Pasture	3	152359	152359	0	41.5079	41.5079	0.383737	1.24069	58465.8	0.619465	18.8813
3	CRP	4	160257	160257	0	38.4666	38.4666	0.252299	0.855599	40432.7	0.502294	15.3099
4	Timber	5	121869	121869	0	106.069	106.069	0.71515	2.79821	87154.6	0.845665	25.7759
5	Wildlife/Wooded	6	1825	1825	0.00001	7.3607	7.36069	0.965743	1.03896	1762.48	0.982722	29.9534
6	Road	7	44609	44609	0	107.915	107.915	0.318614	0.942917	14123.9	0.562685	17.1506
7	Row Crop	8	353980	353980	0	328.666	328.666	0.214536	0.903116	75941.3	0.463180	14.1177
8	Alfalfa	9	9979	9979	0	8.07532	8.07532	0.179604	0.476496	1792.27	0.423797	12.9173
<b>TOTALS</b>			<b>907612</b>							<b>295399</b>		
<p><b>Mean Squ. Difference = 295399/907612 = .3255</b></p> <p><b>Square root of MSD = .5705</b></p> <p><b>RMSE = .57' or 17.4 cm</b></p>												

**Fig. 10.** Root mean square error (RMSE) calculation of photogrammetrically derived DEM and LiDAR DEM, after 2000–2005 change areas have been removed from the calculation. Area field is m<sup>2</sup>.

of the aerial photography flight in 2000 and the LiDAR flight in 2005. These changes mainly included areas where the installation of sediment retention structures and dams, and road grading, had occurred. When these areas were digitized and

excluded from the squared difference calculation, the overall RMSE was found to be 0.57 ft or 17.4 cm (Fig. 10). The RMSE of the row crop area was 0.46 ft (14.3 cm), the grass areas 0.62 ft (18.9 cm) and forested areas 0.85 ft (25.8 cm).



**Fig. 11.** Portion of a shaded relief image made from a NED 30 m DEM. The area is from the Lake Darling watershed in Washington County, Iowa.

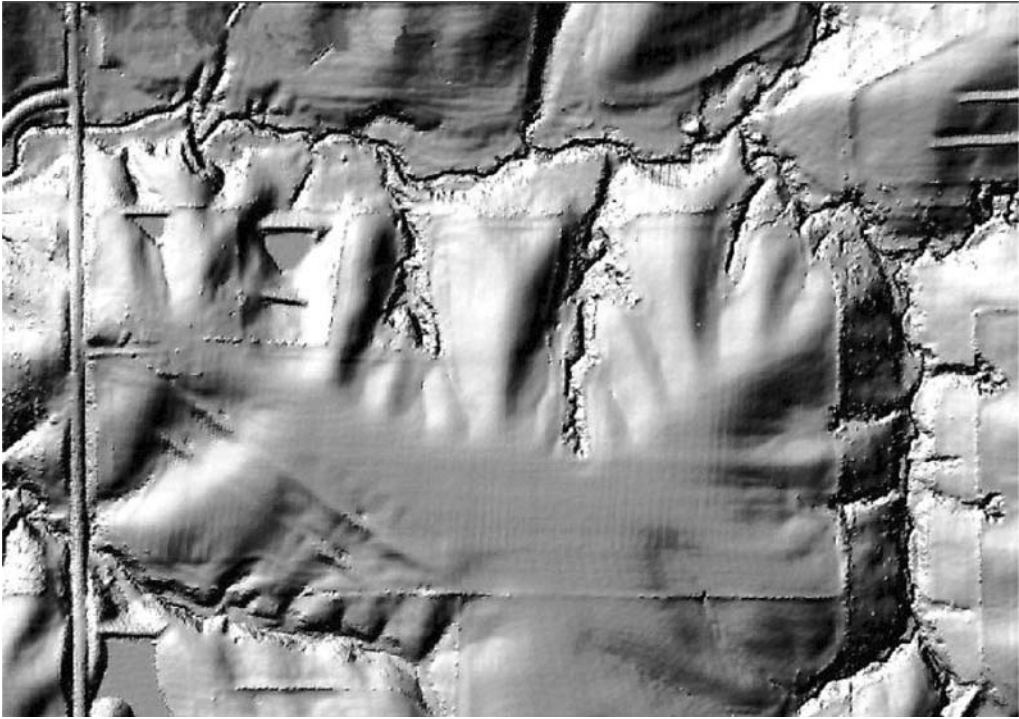


**Fig. 12.** Portion of a shaded relief image made from a 1 m LiDAR DEM for the same area as Figure 11 in Washington County, Iowa.

If the DEM derived by photogrammetric means is accepted as the higher accuracy source, then the LiDAR meets its stated accuracy of 15 cm in the bare ground areas and less than 37 cm in the vegetated areas. This appears to be a good test of LiDAR accuracy because it includes many types of land cover conditions, not just a few high accuracy locations at benchmarks on roads or nearby ditches.

### Comparing old and new data

One of the first tests of any new LiDAR dataset is to compare it with the existing DEM derived from the 10 ft contours of the USGS (US Geological Survey) topographical quadrangle mapping projects of the latter half of the twentieth century. Displayed at smaller scales, it is difficult to see much difference between the shaded relief images derived from the 30 m resolution National Elevation Dataset or NED (<http://ned.usgs.gov/>) and LiDAR shaded relief. Only when the display is zoomed into larger scales is it possible to see the marked differences between the 30 m NED (Fig. 11) and LiDAR DEM (Fig. 12). On a large scale, man-made features such as roadways and ditches, fence lines, terraces

and dams are easily seen, as well as natural features such as stream channels, gullies and floodplains. None of these smaller features is discernable on the 30 m NED shaded relief image.

Where LiDAR really excels is in mapping areas with little relief. Figure 13 is a shaded relief image derived from the 30 m NED, which shows typical glaciated terrain in north-central Iowa, east of Spirit Lake in Dickinson County, Iowa. Figure 14 shows the same area using 1 m resolution LiDAR, which focuses the indistinct mounds seen on the NED shaded relief into sharply defined, circular and elongated features. These are interpreted to be the remnants of ice-walled lakes, which were formed on the surface of the last Pleistocene glacier to visit the area. These lakes filled with sediment, leaving the latter as low mounds after the ice had melted (Quade *et al.* 2004).

Figure 15 shows the Missouri River floodplain north of Council Bluffs, Iowa, in a view that again uses the 30 m resolution NED to create a shaded relief image. It reveals numerous defects in the original conversion of widely spaced contours on a very flat surface. With a 10 ft contour interval, there is not enough information to adequately interpolate features on the floodplain. For example, the

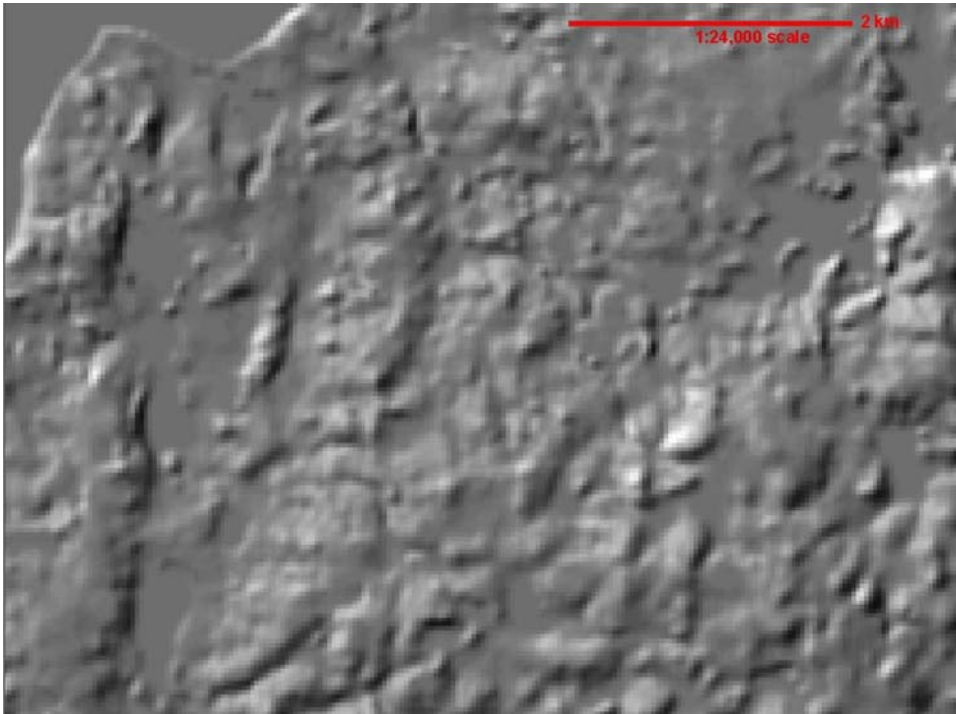


**Fig. 13.** Portion of a shaded relief image showing recently glaciated terrain near Spirit Lake in Dickinson County, Iowa. The shaded relief was created from a 30 m resolution DEM from the NED.

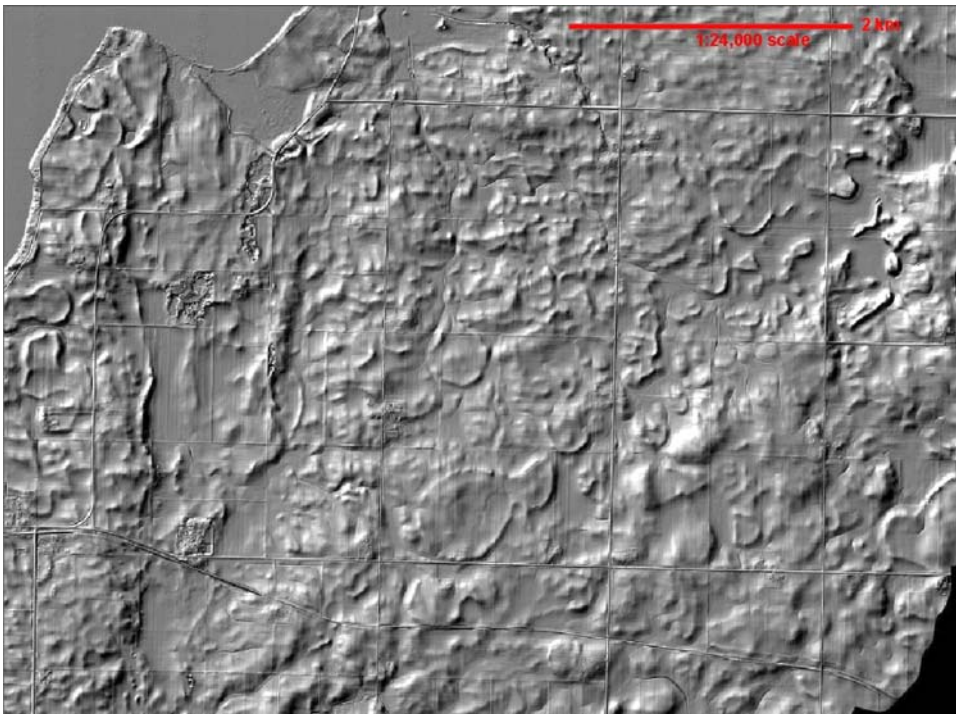


**Fig. 14.** Portion of a LiDAR-derived shaded relief image of the same area of glacial terrain near Spirit Lake in Dickinson County, Iowa. Notice how the shapes of subtle, low relief glacial features are now readily apparent.

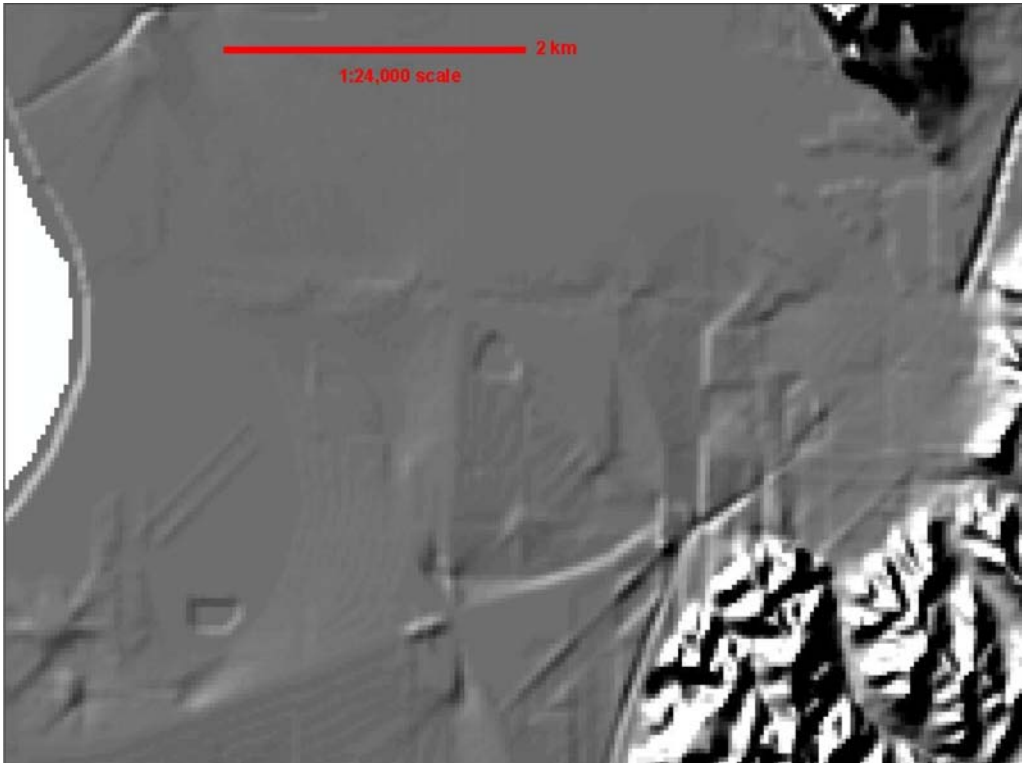


**Fig. 15.** Portion of a shaded relief image showing the Missouri River floodplain north of Council Bluffs, Iowa. The shaded relief image was created from a 30 m resolution DEM from the NED. Notice the cross-shaped features that are artefacts of the interpolation of the original 10 ft contours from USGS topographical maps.

shaded relief image reveals cross-shaped artefacts within the DEM, which were created by the interpolation software trying to connect widely spaced data. Figure 16 shows the great improvement afforded by interpolating a surface from closely spaced LiDAR points (about 2 m LiDAR point spacing). The features revealed on the LiDAR shaded relief image include: Missouri River meander scars, levees along drainage ditches, fence lines, interstate lanes, railroad right of ways, borrow pits and sewage lagoons.

Geological mappers using shaded relief images for on-screen digitizing will need to learn new techniques of recognizing and separating man-made as well as geomorphic features. Because shaded relief images can represent the encoding of relatively small changes in slopes, mappers will need to build up criteria for the recognition of everyday features using the clues in contrast, shading, shape, texture, pattern and context contained in these images. This contrasts with past practices in which geological mappers interpreted aerial photographs by poring over example after example of

natural and man-made features, and learned how to interpret geological features by looking at their geomorphic signatures on topographical maps. LiDAR will cause us to relearn and reinvent both techniques by moving the geomorphic scale down to the realm of the air photograph, roughly at resolutions from 1 to 5 m. While qualitative information on slopes was formerly available through the use of stereo viewers and aerial photographs, only now, with the advent of LiDAR data, is there so much quantitative slope information available. With digital elevation data derived from LiDAR, new computer-assisted classification strategies can be developed for geomorphic features, as well as developing new types of imagery to support manual interpretations.

### Summary

Large-scale LiDAR acquisitions will provide mapping professionals with an abundance of new high-quality elevation data to use as base maps for



**Fig. 16.** Portion of a LiDAR-derived shaded relief image of the same area on the Missouri River Floodplain. Notice the much finer detail showing the interstate cloverleaf, river meander scars, borrow pits, and a ditch and levee system. Editing by the vendor removed the bridge deck. LiDAR DEM obtained from the Pottawattamie County GIS Department.

their projects. To take full advantage of this new data source, those carrying out the mapping need to be aware of how LiDAR data are collected, and the type of data reduction processes that are used by commercial vendors to make deliverable products for their clients. In many cases, mappers will want to manipulate the raw LiDAR returns into their own TINs, DEMs and derived products, but sometimes they will only have access to vendor-supplied finished products that have undergone unknown procedures to make the visual appearance more appealing. Mappers can use shaded relief images derived from LiDAR DEMs or TINs for on-screen digitizing, as well as new derivative products such as terrain slope and LiDAR intensity to identify geological and other features. The new generation of LiDAR data users will be interested in the absolute

vertical accuracy of elevations and will need to know how land cover type affects that accuracy.

## References

- BALTSAVIAS, E. P. 1999. Airborne laser scanning: basic relations and formulas. *ISPRS Journal of Photogrammetry and Remote Sensing*, **54**, 199–214.
- QUADE, D. J., GIGLIERANO, J. D. & BETTIS, E. A. III 2004. Surficial geologic materials of the Des Moines Lobe of Iowa, Phase 6: Dickinson and Emmett Counties: IDNR/IGS, OFM-0402, 1:100 000 scale. Available online at: <http://www.igsb.uiowa.edu/gsbpubs/pdf/ofm-2004-2.pdf>.
- WEHR, A. & LOHR, U. 1999. Airborne laser scanning – an introduction and overview. *ISPRS Journal of Photogrammetry and Remote Sensing*, **54**, 68–82.